Available online at www.sciencedirect.com
ScienceDirect
Journal of the European Ceramic Society 28 (2008) 217–222
www.elsevier.com/locate/jeurceramsoc

Gelcasting of alumina foams consolidated by epoxy resin

Xiaojian Mao [a,b], Shunzo Shimai [a], Shiwei Wang [a,*]

[a] *Shanghai Institute of Ceramics, Chinese Academy of Sciences, Shanghai 200050, PR China*
[b] *Graduate School of Chinese Academy of Science, Beijing 100039, PR China*

Received 12 April 2007; received in revised form 15 June 2007; accepted 21 June 2007
Available online 20 August 2007

Abstract

A water-soluble epoxy resin combined with a polyamine hardener was developed to consolidate foamed suspensions to manufacture alumina foams. This gelling system could be carried out in air atmosphere, thus more convenient than those based on acrylamide derivatives. The influence of solid loading on the viscosity of suspensions as well as on the relative density of sintered foams was evaluated. The resulting alumina foams, with relative densities between 17% and 38%, comprised microstructures of spherical cells. Both the flexural strength and the compressive strength of the foams had a power law relation against the relative density. The permeability of sintered foams decreased exponentially with the relative density.

Keywords: Porosity; Foams; Strength; Al_2O_3; Suspension; Gelcasting

1. Introduction

Porous ceramics have been widely used in many industrial applications, such as filters for molten metals, catalyst carriers for chemical plants and automobiles, furnace linings, lightweight structural materials, biomaterials and so on.[1–4] Several technologies were developed to manufacture strong and reliable porous ceramics. Among them, gelcasting of foams is of important advantages in the production of macroporous ceramics.[5] This technology combines the foaming of suspensions and the *in situ* polymerization for setting the liquid foam. Such a process yields cellular structures with porosity varying from 40% to >90%, with pores closed or open, depending on pore fraction. Mechanical strength of sintered foams was higher than that obtained by other routes, because of the spherical pore shape associated with a fully densified matrix.[6]

However, the usual monomers are acrylamide derivatives, and the polymerization is a free radical reaction, which is inhibited by oxygen. For example, just 0.2% oxygen was sufficient to inhibit the reaction completely in foamed suspensions.[7] Thus, the foaming and polymerization procedures have to be carried out in a N_2 filled chamber to insulate oxygen. However, a technical process under nitrogen is complicated, and hence increases the cost of production, especially taking industrial production into consideration. It is an available and feasible way to develop new monomer systems, which could be carried out in air atmosphere to resolve this problem substantially.

On the other hand, some polymers, such as cellulose derivatives, polysaccharides, alginates and proteins, which may gel in atmosphere, have worked successfully in the production of dense components. However, difficulties regarding fluidity of slurries and insufficient strength for handling green bodies discourage their continued applications.[5]

Recently, our study has developed a water-soluble epoxy resin as gelling agent for gelcasting of ceramics in air atmosphere.[8] Presently, it was exploited to consolidate foamed suspensions with a polyamine hardener to manufacture alumina foams.

2. Experimental procedure

2.1. Materials

A commercial alumina powder (AES-11, Sumitomo Chemical Co., Ltd., Tokyo, Japan), with an average particle size of 0.45 μm and a specific surface area of 6.4 m^2/g, was used as

* Corresponding author. Tel.: +86 21 52414320; fax: +86 21 52413903.
E-mail address: swwang51@mail.sic.ac.cn (S. Wang).

0955-2219/$ – see front matter © 2007 Elsevier Ltd. All rights reserved.
doi:10.1016/j.jeurceramsoc.2007.06.006

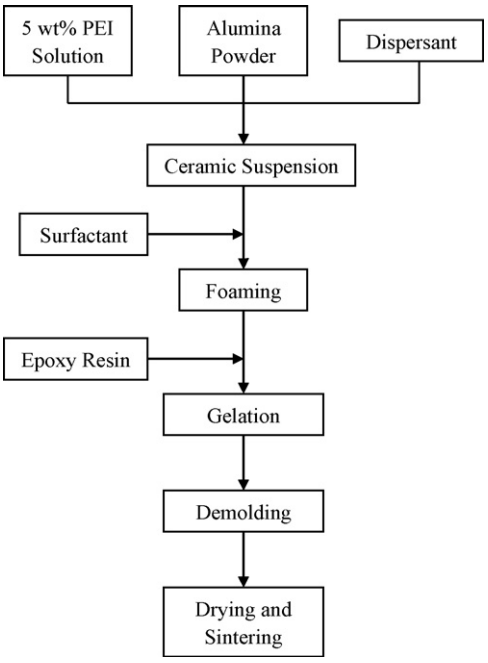

Fig. 1. Flow-chart for production of ceramic foams by foaming and gelation.

raw material. Polyacrylic acid ammonium salt (A-30SL, 40% in water, Toa Gosei Co., Tokyo, Japan) was selected as the dispersant. A commercial surfactant solution Triethanolamine lauryl sulfate (with 40% active content, Emal TD, Kao Chemical Co., Tokyo, Japan) was used as foaming agent. An epoxy compound sorbitol polyglycidyl ether (SPGE) (Nagase Chemtex, Osaka, Japan), whose epoxy equivalent weight is 173 g/epoxy equivalent, and a polyamine hardener polyethyleneimine (PEI) (30% in water, Tokyo Kasei Kogyo Co., Ltd., Tokyo, Japan) were employed to consolidate liquid foams.

2.2. Alumina foams production

Fig. 1 is the flowchart for fabricating alumina foams. PEI was first diluted in deionized water to obtain 5 wt.% premix solution. Aqueous suspensions with solids loading of 60–76 wt.% were prepared by ball-milling alumina powder, dispersant and the premix solution. The rheological properties of the suspensions were measured by a stress-controlled rheometer (Model SR5, NJ) within the shear rate range of 1–1000 s^{-1}. To generate foams, vigorous stirring about 5 min was applied after adding the surfactant. For setting the fluid foams, 10 wt.% SPGE based on the premix solution was added with further stirring about 30 s. The foamed suspensions were immediately poured into plastic molds and sealed at room temperature for 1 h. To characterize the gelling behavior of the system, aqueous solution and foamed suspension were subjected to sinusoidal oscillation at a continuous frequency of 1.0 Hz and a constant strain, γ_0, of 0.4% after adding SPGE. During this operation the responding stress, σ_0, was measured. The calculated storage modulus, G', is given by

$$G' = \frac{\sigma_0}{\gamma_0 \cos \delta} \quad (1)$$

where δ is the phase angle between the stress and the strain.[9] Wet green bodies were demolded and moved to a drying chamber for 24 h, in which the relative humidity was above 95% and the temperature was 60 °C. After that, these green bodies were placed to an oven of 120 °C for complete dry. The binder burn-out profile of the dried body was obtained by differential thermal analysis (DTA) and thermogravimetric analysis (TGA) in air at a heating rate of 10 °C/min on Netzsch STA 449C equipment. Finally, sintering was performed at 1650 °C for 2 h using a heating rate of 1.5 °C/min to 600 °C and then 3 °C/min to 1650 °C.

2.3. Characterization of the foams

The relative densities of alumina foams were determined in terms of the ratio of mass to volume. Both flexural strength and compressive strength were examined using an Instron-5566 universal testing machine at a loading rate of 1 mm/min. The sample dimension for flexural strength was 5 mm × 10 mm × 50 mm, and for compressive strength was 15 mm × 15 mm × 15 mm. The microstructures of alumina foams were observed by scanning electron microscopy (SEM, JSM-5600LV, Japan). Cell size distribution was obtained using an image analyzer (Leiea Qwin). To calculate gas permeabilities, the pressure drops of disk-shaped specimens (φ: 30 mm × 5 mm) were measured with increasing volumetric flow rate of N_2 gas in the range of 10–1000 L/h.

3. Results and discussion

3.1. Rheology of suspensions

Fig. 2 shows the rheological flow curves of suspensions with different solid loadings. It can be seen that all the suspensions prepared in this work revealed a shear thinning or pseudoplastic behavior and the viscosity increased with solid loading at the measured shear rate range. This phenomenon was similar to those of suspensions with high alumina content.[8,10,11] In the fabrication of ceramic foams, it was considered[10] that a slight

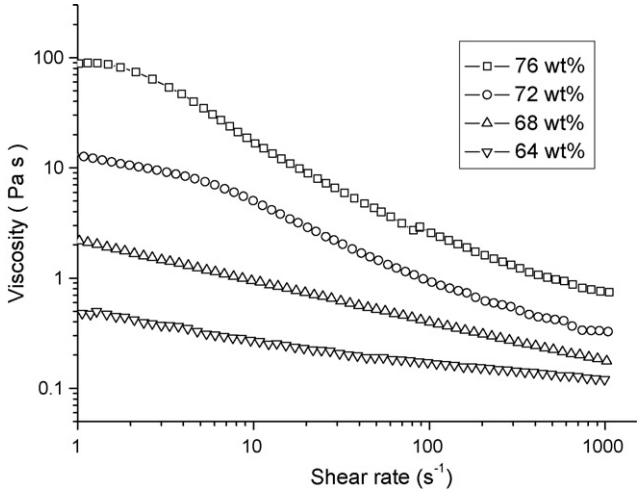

Fig. 2. Rheological flow curves of suspensions with different solid loadings.

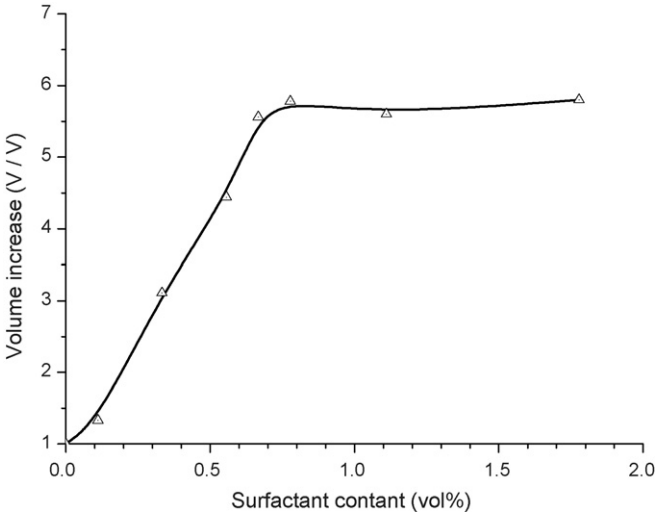

Fig. 3. Evolution of the foaming capacity versus the concentration of the surfactant.

pseudoplasticity could favor the generation of foams since lower viscosities were obtained under shearing, and could significantly improve the foam stability under static conditions since the viscosity increase delayed the collapse of fluid films around the bubbles.

3.2. Foaming of alumina suspensions

Fig. 3 shows the effect of surfactant concentration on the foaming capacity of the suspension with 70 wt.% solid loading. The foaming capacity is evaluated in terms of the volume ratio of foamed suspension to the original one. As the surfactant content was increased to 0.7 vol.%, the volume of foamed suspension was 5.8 times of that of original one, and remained at this level with further increasing the surfactant content. It could be explained that increasing the surfactant content favors the adsorption at the gas/liquid interface and decrease of the surface tension, which will favor foaming. For a higher concentration of 1.0 vol.%, for example, the surface tension remains minimal value, hence the foaming capacity keeps steady. From Fig. 3, the surfactant addition of 0.8 vol.% of suspension was optimized for other foaming process.

3.3. Consolidation of the system

The changes of G' and $\tan\delta$ during gelation are shown in Fig. 4. The storage modulus represents the elastic component of a system, while $\tan\delta$ denotes the ratio of the loss modulus (G'') to the storage modulus. For the aqueous solution without adding powders and foaming, the increase of storage modulus occurred at about 10 min, followed by a sustaining increase. Correspondingly, from 10 min on, $\tan\delta$ decreased sharply from about 1.3 to less than 0.1. It could be considered that a three-dimensional network was formed at about 10 min, and consolidated continuously. For the foamed suspension containing 72 wt.% solids, on the other hand, the changes of G' and $\tan\delta$ occurred at the beginning of the measurement. The differences from those of

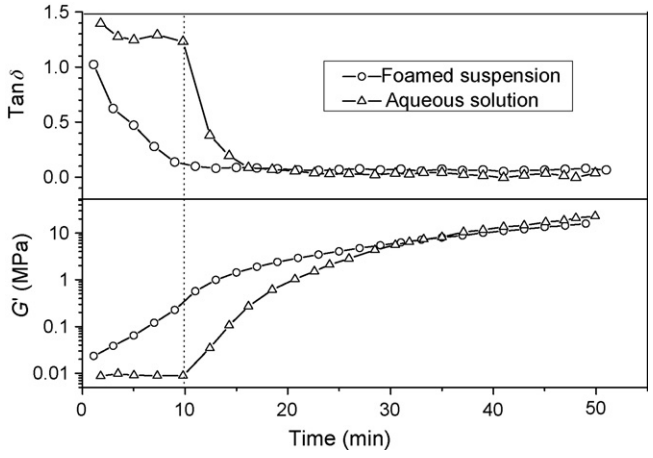

Fig. 4. G' and $\tan\delta$ of aqueous solution and foamed suspension changed with time.

the aqueous solution might attribute to the existence of alumina powders. Although the three-dimensional network was not formed at the beginning of the measurement, the increasing organic molecules, which resulted from the gelling reaction, trapped more and more water. Hence, the interaction between alumina particles was increased, which resulted in the increase of G' and the decrease of $\tan\delta$. So, after adding SPGE and mixing, the foamed suspensions should be cast as soon as possible. In practice, it was favorable in 3 min.

3.4. Burn-out behaviors

The simultaneously traced TG/DTA curves of the dried body are presented in Fig. 5. The dominating weight loss occurred between 240 °C and 580 °C, corresponding to an exothermic peak at about 320 °C. This wide burn-out range allows an easy debindering process. On the other hand, foamed green body is easy to debinder than dense body, for it contains abundant cells and channels to let pyrolysates escape. In present study, a heating rate of 1.5 °C/min was applied successfully to remove the binders without cracks.

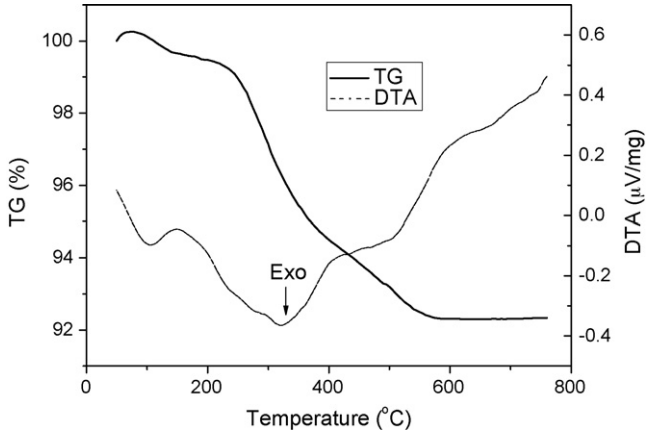

Fig. 5. TG/DTA curves for thermal behavior of dried body in air.

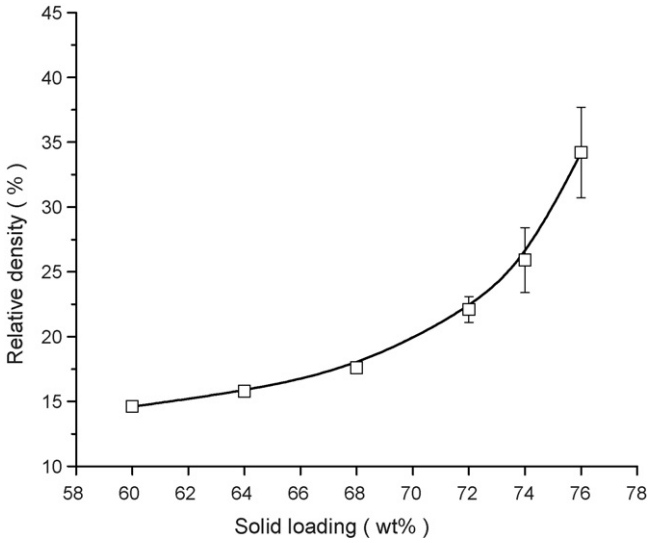

Fig. 6. Relative density of the sintered foams as a function of the solid loading of suspension.

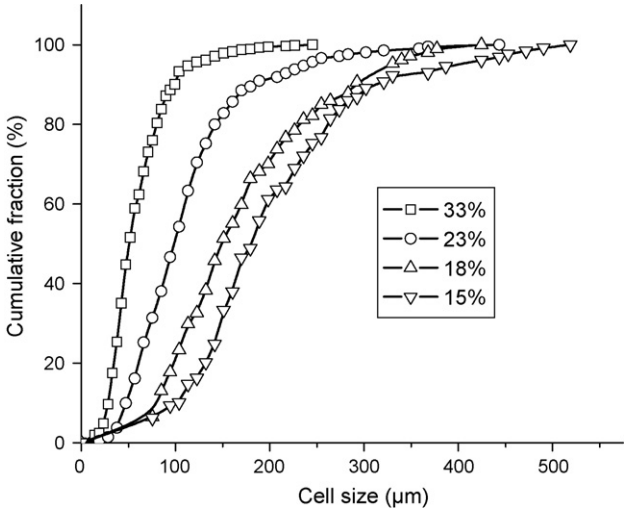

Fig. 8. Cell size distributions of alumina foams with various relative densities.

3.5. Foam density and cell size distribution

Fig. 6 shows the relative density of the sintered alumina foams as a function of the solid loading of original suspensions. It can be seen that the relative density increased with the solid loading while other processing conditions were uniform. It could be considered that high solid loading resulted in high viscosity, which corresponded to low foaming capacity and high relative density. So, the products with different relative densities could be easily obtained and controlled by means of the suspensions with different solid loading.

The density played an important role in determining the microstructure of the sintered foams, as shown in Fig. 7. The foams exhibited approximately spherical cells with no preferred orientation, resulting in isotropic properties, which was a typical result of direct foaming method.[12] It can also be seen that with the decrease of the density the mean cell size and the window size increased.

Fig. 8 shows the cumulative cell size distributions of foams with various relative densities. As the relative density deceased

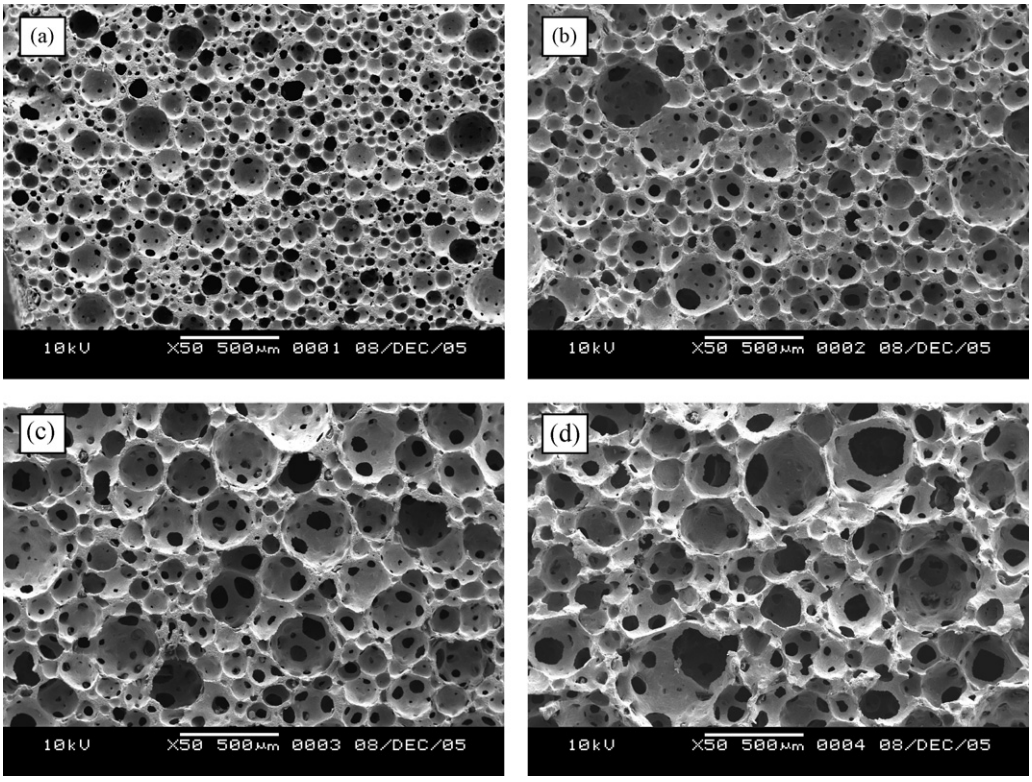

Fig. 7. SEM micrographs of alumina foams with relative densities of (a) 33%, (b) 23%, (c) 18% and (d) 15%.

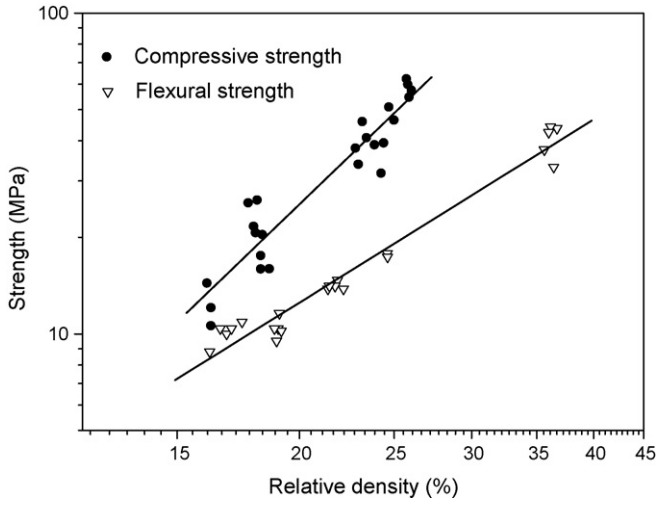

Fig. 9. Flexural strength and compressive strength of alumina foams against relative density.

from 33% to 15%, the average cell size increased from about 50 μm to about 180 μm, and the cell size distribution was widened.

3.6. Mechanical strength

The flexural strength and the compressive strength of alumina foams with various relative densities were presented in Fig. 9. As expected, the strength decreases with decreasing relative density. The power law relation between strength and density proposed by Gibson and Ashby [13] is one of the classic theoretical explanations for brittle cellular solids:

$$\frac{\sigma_{cr}}{\sigma_{fs}} = C_1\left(\frac{\rho}{\rho_s}\right)^{3/2} \quad (2)$$

where σ_{cr} is the brittle collapse stress of foams, σ_{fs} is the modulus of rupture of strut, C_1 is a constant, ρ is the foam density and ρ_s is the strut density. Generally, a similar experiential equation is successfully applied in describing the dependence of the strength on the density of ceramic foams: [6,12,14,15]

$$\frac{\sigma}{\sigma_s} = C_2\left(\frac{\rho}{\rho_s}\right)^{n} \quad (3)$$

where σ is the foam strength, σ_s is the strut strength and n and C_2 are constants. Another simple equation is obtained from Eq. (3):

$$\sigma = C_3{\rho_r}^n \quad (4)$$

where C_3 is a coefficient equivalent to the product between σ_s and C_2, and ρ_r is the relative density. The data in double log plot of Fig. 9 was linearly fitted in terms of Ep. (3). The obtained values of the exponent n in the fitting equation were 1.9 for flexural strength data and 2.9 for compressive strength data. The values are comparable to those of prior publish.[6,12,14,15]

As known to all, compressive strength is much higher than that of flexural strength for dense ceramic materials. However, the data in Fig. 9 revealed that the difference between compressive and flexural strength of the foams decreased as relative density was decreased. It could be explained by Gibson and Ashby' model [13] that the crushing collapse of highly porous brittle foams occurs as a flexural rupture mode and is determined by the modulus of rupture of strut σ_{fs}, not by the compressive strength of strut.

3.7. Permeability

Permeability is one of the important properties for solid foams. Pressure drop increasing proportionally with flow rate in the present study (not presented here) indicated that the relation between pressure drop and flow rate could be described by Darcy's equation:

$$\frac{\Delta P}{L} = \frac{\mu Q}{kA} \quad (5)$$

where ΔP is the pressure drop on sample, L is the sample thickness, A is the flow area through sample, μ is the dynamic viscosity, Q is the volumetric flow rate and k is the Darcian permeability. The calculated values of the Darcian permeability with various relative densities were presented in Fig. 10, using the value of 1.6×10^{-5} Pa s for the dynamic viscosity (μ) of N_2 at room temperature and atmospheric pressure. The permeability of the foams with relative density ranging from 17% to 36% varied between 6×10^{-11} m^2 and 3×10^{-13} m^2. The approximately linear relation between Darcian permeability and relative density in double log plot suggests that it could be described by a referenced power law model as Eq. (4):

$$k = K\rho_r^m \quad (6)$$

where K is a coefficient with the unit of m^2, m is a constant. The obtained values in the fitting equation Eq. (6) were 2.3×10^{-16} m^2 and -7.04 for K and m (with the correlation coefficient of $R = -0.99$), respectively.

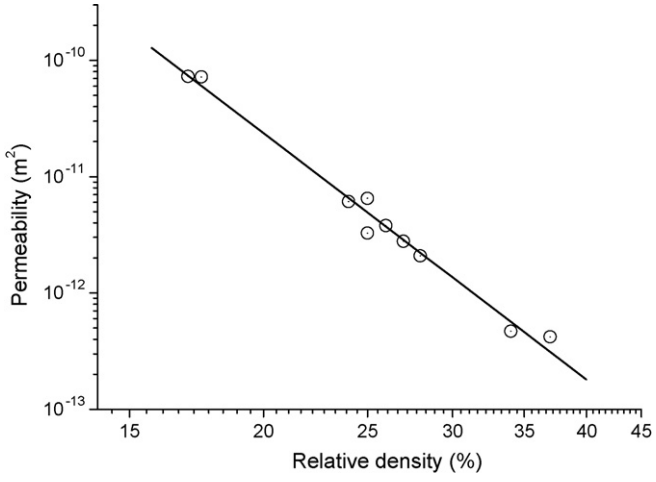

Fig. 10. Permeability of the foams as a function of relative density.

4. Conclusions

A water-soluble epoxy resin (SPGE) combined with a polyamine hardener (PEI) was successfully applied to set foamed suspensions for the production of alumina foams. The advantage of this gelling system is that it could be carried out in air atmosphere. Alumina foams with controlled relative density and cell size distribution were obtained by the approach. Both the flexural strength and the compressive strength of the foams had a power law relation against the relative density, and the calculated power law indexes were 1.9 and 2.9, respectively. The permeability of the foams varied between 6×10^{-11} m^2 and 3×10^{-13} m^2 with relative density ranging from 17% to 36%.

References

[1]. Hirschfeld, D. A., Li, T. K. and Liu, D. M., Processing of porous oxide ceramics. *Key Eng. Mater.*, 1996, **115**, 65–80.

[2]. Liu, D., Preparation and characterization of porous hydroxyapatite bioceramic via a slip-casting route. *Ceram. Int.*, 1998, **24**(6), 441–446.

[3]. Kato, S., Hirano, Y., Iwata, M., Sano, T., Takeuchi, K. and Matsuzawa, S., Photocatalytic degradation of gaseous sulfur compounds by silver-deposited titanium dioxide. *Appl. Catal. B: Environ.*, 2005, **57**, 109–115.

[4]. Nagadomi, H., Takahasi, T., Sasaki, K. and Yang, H. C., Simultaneous removal of chemical oxygen demand and nitrate in aerobic treatment of sewage wastewater using an immobilized photosynthetic bacterium of porous ceramic plates. *World J. Microbio. Biotech.*, 2000, **16**, 57–62.

[5]. Sepulveda, P., Gelcasting foams for porous Ceramics. *Bull. Am. Ceram. Soc.*, 1997, **76**(10), 61–65.

[6]. Sepulveda, P., Ortega, F. S., Innocentini, M. D. M. and Pandolfelli, V. C., Properties of highly porous hydroxyapatite obtained by the gelcasting of foams. *J. Am. Ceram. Soc.*, 2000, **83**(12), 3021–3024.

[7]. Sepulveda, P. and Binner, J. G. P., Evalution of the in situ polymerization kinetics for the gelcasting of ceramic foams. *Chem. Mater.*, 2001, **13**, 3882–3887.

[8]. Mao, X. J., Shimai, S. Z., Dong, M. J. and Wang, S. W., Gelcasting of alumina using epoxy resin as a gelling agent. *J. Am. Ceram. Soc.*, 2007, **90**(3), 986–988.

[9]. Barnes, H. A., Hutton, J. F. and Walters, K., *Rheology of suspensions. In An introduction to rheology*. Elsevier, Amsterdam, 1993, pp. 37–54, Chap. 3.

[10]. Sepulveda, P. and Binner, J. G. P., Processing of cellular ceramics by foaming and *in situ* polymerization of organic monomers. *J. Eur. Ceram. Soc.*, 1999, **19**, 2006–2059.

[11]. Ortega, F. S., Valenzuela, F. A. O., Scuracchio, C. H., and *et al.*, Alternative gelling agents for the gelcasting of ceramic foams. *J. Eur. Ceram. Soc.*, 2003, **23** (1), 75–80.

[12]. Colombo, P., Ceramic foams: fabrication, properties and applications. *Key Eng. Mater.*, 2002, **206–213**, 1913–1918.

[13]. Gibson, L. J. and Ashby, M. F., *Cellular Solids: Structure and Properties* (*2nd ed.*). Cambridge, UK, 1997, pp. 210–211.

[14]. Takahashi, R., Sato, S., Sodesawa, T. and *et al.*, Bending strength of silica gel with bimodal pores: effect of variation in mesopore structure. *Mater. Res. Bull.*, 2005, **40**, 1148–1156.

[15]. Oliveira, F. A. C., Dias, S., Fátima, M. and Fernandes, J. C., Behavior of open-cell cordierite foams under compression. *J. Eur. Ceram. Soc.*, 2006, **26**, 179–186.